Int. J. Heat Mass Transfer. Vol. 36, No. 7, pp. 1827–1832, 1993
Printed in Great Britain

0017-9310/93 $6.00 + 0.00

Heat transfer characteristics of a cranked, evaporative thermosyphon

G. S. H. LOCK and JIALIN FU
Department of Mechanical Engineering, University of Alberta, Edmonton, Alberta, Canada, T6G 2G8

(*Received* 13 *January* 1992 *and in final form* 10 *August* 1992)

Abstract—The paper presents an exploratory study of an offset, evaporative thermosyphon. Laboratory experiments using a small bore rig were conducted for a cranked configuration with the evaporator and condenser aligned vertically. Heat transfer data revealed similarities with the equivalent linear system but also showed up some differences. The heat transfer rates were found to be much higher than those obtained under single-phase conditions. On the other hand, critical heat fluxes were much lower than in the equivalent linear system. Various temperature parameters are discussed.

1. INTRODUCTION

DEVELOPMENT of northern regions depends to a large extent on our ability to construct and maintain various engineering structures e.g. buildings, towers, roads, airstrips, etc. Frequently, these structures are built on permafrost which may be subject to thermal erosion or degradation. To help offset this difficulty, various types of cryosyphon have been employed [1]. For the most part, these devices are thermosyphons which use cold winter air to withdraw heat from the soil and thus maintain it in a frozen and subcooled state. During the summer period they automatically shut down and thus help delay, if not prevent, any thawback.

In more southerly climates, the power and process industries have a widespread need for devices which are capable of transferring heat from a hot fluid to a cold fluid. These fluid streams may or may not be immediately adjacent to each other. In any event, the various forms of heat exchanger used to solve this problem can often benefit from alternative, more flexible, heat transfer schemes. Thermosyphon tube bundles may provide such flexibility. This is especially true in waste heat recovery, for example, where retrofit is frequently an important feature of the design.

In a typical application, the thermosyphon is simply a tube enclosing a fluid which circulates under the influence of thermally induced buoyancy forces. It is this circulation which creates the longitudinal convective flux within the tube and thus gives the device its characteristic effectiveness. The buoyancy forces are of two types which may operate separately or jointly. Temperature variations throughout the fluid produce thermal buoyancy under single-phase conditions; the density difference associated with change of phase produces Archimedean buoyancy under evaporative conditions.

Until recently, the vast majority of thermosyphon studies concentrated on the linear tube. Most of this work deals with a vertical orientation but some studies have been undertaken on tilted tubes [2–3]. While there are many applications for which a linear, vertical tube is suitable, it is clear that designers will have much greater flexibility if this geometrical restriction is lifted. For example, a variety of different configurations have been suggested for freezing around piles [4]; a similar observation applies to various shipboard surfaces which may be equipped with thermosyphon de-icers [5].

From the many possibilities, the cranked thermosyphon appears to be among the least studied, even though it is already in use [4, 6]. To remedy this deficiency, an experimental study of the single-phase, cranked thermosyphon was conducted [7]. The present study extends this work to the evaporative, cranked thermosyphon depicted in Fig. 1. As indicated, the device consists of a vertical condenser standing above a vertical evaporator, the two being connected with a horizontal, adiabatic section. For comparative purposes, the geometry of the tubes has been kept the same as in the single-phase experiments.

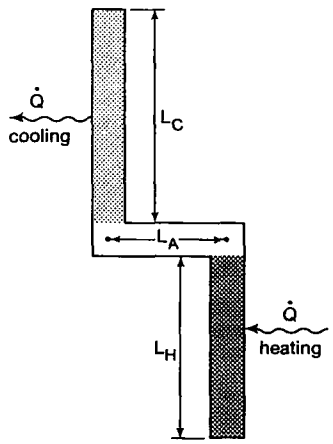

FIG. 1. Schematic of a cranked, tubular thermosyphon.

NOMENCLATURE

A	heated surface area
Ar	Archimedes number
c_p	specific heat
D	tube diameter
g	gravitational acceleration
h	heat transfer coefficient
k	thermal conductivity
K	thermal conductance
Ja	Jakob number
Nu	Nusselt number
Pr	Prandtl number
$\dot{q}$	heat flux density
$\dot{Q}$	heat flux
T	temperature.

Subscripts

C	condenser
H	evaporator
R	reference
I	liquid–vapour interface
T	triple point.

Greek symbols

η	resistance ratio
θ	overall temperature difference
κ	thermal diffusivity
λ	latent heat of evaporation
ν	momentum diffusivity
ρ	density.

2. THE EXPERIMENTS

A schematic of the test rig is shown in Fig. 2. The evaporator consisted of an 80 cm long copper tube, 2 cm diameter. It was sectioned into four 20 cm lengths each with its own heater. The heaters were formed from a length of electrically-resistive tape wrapped around the outside of the copper tube; an asbestos sheath enclosing the tape ensured that it would remain electrically insulated from the tube under high temperature conditions. The heater wires were connected in parallel, thus giving independent control over the local heat flux density (and temperature) along the tube wall. A thick layer of thermal insulation was then wrapped on the outside of the heater wire, thus reducing heat loss to the surrounding atmosphere.

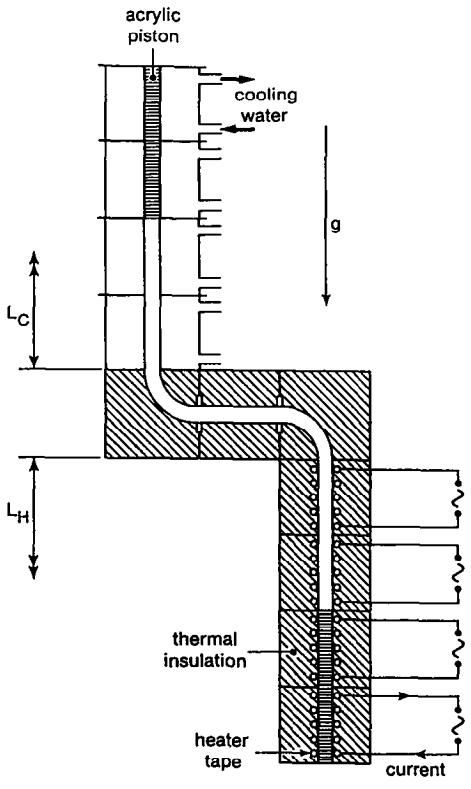

FIG. 2. Schematic of rig.

The condenser was also constructed from an 80 cm long copper tube of the same diameter. This too was sectioned into four 20 cm lengths each with its own cooling jacket. The cooling jackets were fed with water from a copper distribution heater around which was wrapped another heater tape. The building mains supplied the header with water. By this means, the local condenser wall temperature could be regulated to ensure a close approximation to isothermal conditions.

Between the evaporator and condenser was a horizontal tube of the same diameter; this offset piece had a length of 8 cm, measured between the vertical tube axes. It was joined to the vertical tubes by means of flanges attached to bends of radius 6 cm. During the experiments, this offset length was wrapped with thermal insulation to approximate an adiabatic condition.

The electrical power supplied to the evaporator heater was measured in the usual way with an ammeter and voltmeter. The heat lost to the atmosphere was determined from a calibration run in which the evaporator was first filled with thermal insulation. The heat then supplied was plotted against the difference between the tube wall temperature and the ambient temperature. During the experiments proper, this heat leakage was subtracted from the gross supply rate.

Temperatures were measured with copper–constantan thermocouples positioned every 4 cm along the evaporator and condenser walls. A thermocouple was also located in the room air. Signals from the thermocouples were channeled through a switching box and read on a digital multimeter. Saturation tem-

perature was obtained from the measured vapour pressure and the saturation curve.

Before beginning the test runs, the apparatus was first cleaned and charged. The cleaning consisted of bathing the tube surfaces in benzene, followed by alcohol, followed by distilled water, the working fluid. Assembly of the apparatus with 40 cm evaporator and condenser lengths was then completed and a vacuum pump connected. The internal pressure, measured with a Marsh vacuum gauge, was lowered to around 1 kPa at which point the pump was shut off and the apparatus and allowed to sit for several hours in order to detect any leaks. Once leaks, if any, had been removed, a quantity of distilled water was measured and introduced using a hypodermic syringe. For these experiments the charge was fixed at 35% of the evaporator volume. The vacuum pump was again switched on and, in the presence of boiling in the evaporator, used to remove remaining air. The apparatus was then sealed and the experiments begun.

The experimental procedure was as follows. The condenser cooling water was turned on, followed by the power to the evaporator. Once the evaporator wall temperature had been set at a convenient value, a series of data points were collected, each for a different condenser wall temperature. Power supply rate was recorded along with temperatures along the tube walls, in the vapour and in the room. The procedure was then repeated with the evaporator wall temperature at a new level. The range of temperatures covered was as follows: $30\,\text{C} < \theta < 72\,\text{C}$, $61\,\text{C} < T_H < 112\,\text{C}$, $25\,\text{C} < T_C < 47\,\text{C}$ and $37\,\text{C} < T_l < 57\,\text{C}$. The last of these, the saturation temperature range, indicates that the tests were all conducted with subatmospheric pressures.

3. DISCUSSION OF RESULTS

3.1. *Analytical framework*

The heat transfer rate $\dot{Q}$ through a thermosyphon may be described [8] by the relation

$$\dot{Q} = Q_1(T_H, T_C) \tag{1a}$$

where T_H and T_C are the heated and cooled wall temperatures, respectively; in general, these are *independent* variables. Alternatively, we may take

$$\dot{Q} = Q_2(\theta, T_R) \tag{1b}$$

where $\theta = T_H - T_C$ and $T_R = t(T_H, T_C)$ is a convenient, single-valued function which, together with θ, prescribes T_H and T_C, and hence $\dot{Q}$. Using equation (1b), it follows that

$$d\dot{Q} = \left(\frac{\partial Q_2}{\partial \theta}\right)_{T_R} d\theta + \left(\frac{\partial Q_2}{\partial T_R}\right)_{\theta} dT_R$$

which reduces to

$$\dot{Q} = \int_0^{\theta} f(\theta, T_R)\, d\theta \tag{2}$$

where

$$f(\theta, T_R)\left(\frac{\partial Q_2}{\partial \theta}\right)_{T_R},$$

only if

$$\left(\frac{\partial Q_2}{\partial T_R}\right)_{\theta} = 0,\ dT_R = 0,$$

or both.

Under such conditions, the thermal conductance of the device

$$K = hA = \frac{1}{\theta}\int_0^{\theta} f(\theta, T_R)\, d\theta \tag{3}$$

is seen to be the thermally averaged value of f. Should f be independent of θ, equation (2) reduces further to

$$\dot{Q} = f(T_R)\theta. \tag{4}$$

With these restrictions understood, equation (4) yields

$$\dot{q} = f(T_R)\frac{\theta}{A} \tag{5}$$

where A is the heated surface area, and

$$h = \frac{f(T_R)}{A}. \tag{6}$$

Under single-phase conditions, T_R is conveniently taken as the mean temperature $(T_H + T_C)/2$ at which fluid properties are evaluated [7]. Under evaporative conditions, T_R is more logically taken as the saturation temperature T_l at the liquid–vapour interface. However, there are many other possibilities, two of which are discussed below.

3.2. *Performance characteristics*

Figure 3 shows a plot of heat flux density $\dot{q}$, based on heated surface area, plotted against the overall

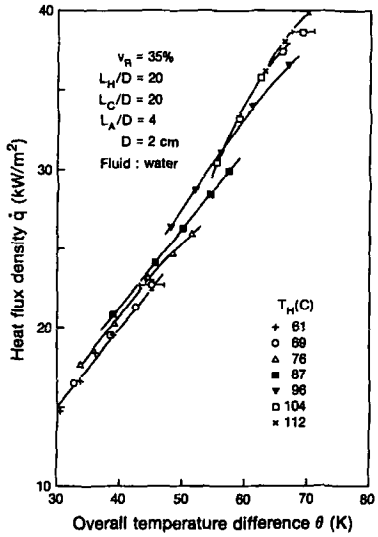

FIG. 3. Heat transfer in an evaporative, cranked thermosyphon standing vertically.

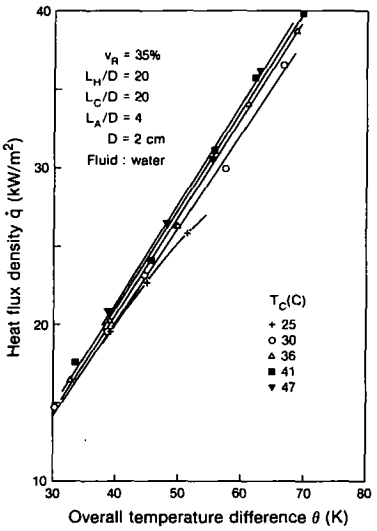

FIG. 4. Effect of condenser temperature on heat transfer in an evaporative, cranked thermosyphon.

temperature difference θ with T_R equal to the evaporator wall temperature T_H. As indicated, the curves are essentially linear, and thus the conditions leading to equation (5) are met, implying that the range of T_H and its independent effect on heat flux are both very small; they occur as a product and therefore reinforce each other. This choice of $T_R = T_H$ is appropriate to thermosyphon data developed for an isothermal heat source. When the application is to an isothermal heat sink, $T_R = T_C$ is more appropriate [8]. Figure 4 provides the alternative plot and reveals similar behaviour.

As noted above, a useful thermal parameter in evaporative systems is $T_R = T_I$. The corresponding presentation is given in Fig. 5. Given that $T_C < T_I < T_H$, it is not surprising that the form of the data is very

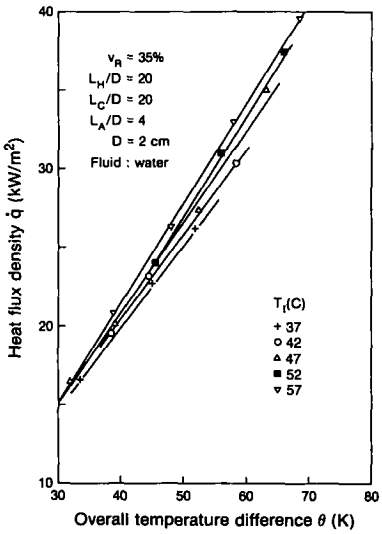

FIG. 5. Effect of vapour temperature on heat transfer in an evaporative, cranked thermosyphon.

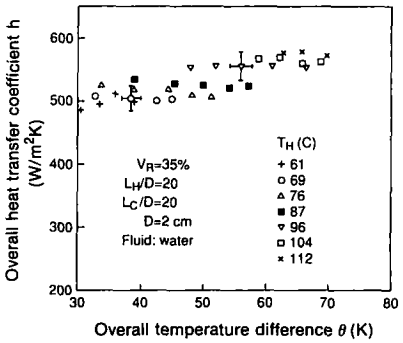

FIG. 6. Overall heat transfer coefficient in an evaporative, cranked thermosyphon.

similar to that seen in Figs. 3 and 4. This form has the advantage that it uncovers the effect of system pressure by making use of the Clausius–Clapeyron equation, but carries the disadvantage that it requires additional processing of the data. Plots of T_I vs T_C for each of the iso-T_H curves obtained experimentally were found to be nonlinear, thus precluding the use of a simple interpolation formula. Instead, the iso-T_I curves were constructed graphically. In general, it is easier to construct them from the iso-T_H and iso-T_C data than to obtain them directly from experiment.

Each of the above three figures reflects the form of equation (5) and thus suggests that each could easily be converted into conductance or heat transfer coefficient data. Figure 6 presents the data with $T_R = T_H$ using the heat transfer coefficient as the dependent variable. In fact, h is essentially independent of θ, as required by equation (6) when f is independent of θ. As expected, $f(T_H)$ is seen to be a monotonically increasing, but weak, function of T_H.

Overall performance integrates the behaviour of the evaporator and condenser but does not provide any details of their behaviour individually. Some insight may be obtained by calculating the ratio of their internal thermal resistances defined by

$$\eta = \frac{T_I - T_C}{T_H - T_I}. \tag{7}$$

This is shown plotted against the overall temperature difference in Fig. 7. As indicated, the ratio is less than

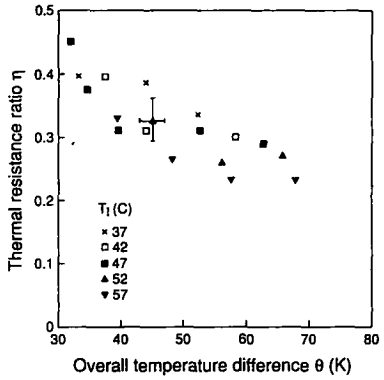

FIG. 7. Thermal resistance ratio in a cranked, evaporative thermosyphon.

1.0, thus signalling to the designer that the evaporator offers the greater opportunity for performance improvement, especially at higher values of heat flux. Given the uncertainty shown, the effect of saturation pressure is evidently quite small, at least in the range studied.

In the light of the thermal resistance measurements, it is interesting to explore the relation

$$Nu_D = f\left(\frac{Pr\,Ar_D}{Ja}\right) \tag{8}$$

where $Nu_D = hD/k$, $Pr = \nu/\kappa$ is the Prandtl number, $Ar_D = gD^3\Delta\rho/\rho\nu^2$ is the Archimedes number and $Ja = c_p\theta/\lambda$ is the Jakob number. The classical form of this equation for film condensation is a simple power law relation [8]. The power is positive for laminar conditions and negative for turbulent conditions. Figure 8 shows representative data plotted on logarithmic scales using the nondimensional interface temperature $(T_I - T_T)T_T$ as a parameter. This again reveals only a small interfacial temperature and pressure effect. It is also evident that for the conditions studied

$$Nu_D = 41.7\left(\frac{Pr\,Ar_D}{Ja}\right)^{-1/5}. \tag{9}$$

This result suggests that the system as a whole is turbulent. Such behaviour is not unexpected in the evaporator, which has the dominant resistance, but appears to include the stratified flow in the offset length and also extends into the condenser.

3.3. *Comparisons*

Auxiliary experiments with the evaporator and condenser axes aligned coincidentally and vertically, showed that the effect of the offset on heat transfer rate was negligible, at least for this particular length and filling quantity. This is a promising result for the designer seeking greater flexibility. Only at the highest values of θ was the offset system limit reached. Based on the periodic wall temperature excursions then observed in the upper reaches of the evaporator, this limit evidently corresponds to flooding and holdup, a condition that is exacerbated by the poorly draining, horizontal offset length. The critical heat transfer coefficients were well below those measured by Imura *et al.* [9] using water in a similar, though linear, arrangement. However, they were significantly higher than those obtained under single-phase conditions; typically, the evaporative system was an order of magnitude better than the non-evaporative system with the same fluid and geometry [7].

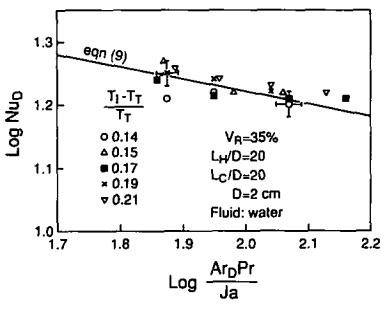

FIG. 8. Nondimensional heat transfer relation for a cranked, evaporative thermosyphon.

Experiments with the evaporator and condenser aligned horizontally, the latter being directly above the former, showed a dramatic change in behaviour. Under these conditions, it appeared that holdup in the condenser coupled with dryout in the evaporator rendered the device virtually inoperative. This stands in sharp contrast to the behaviour of the single-phase equivalent which exhibits substantial improvements in the heat transfer rate when in the horizontal position [10].

4. CONCLUSIONS

The paper has given a discussion of the performance of an offset, evaporative thermosyphon aligned vertically. Using the same geometry and configuration employed previously under single-phase conditions, consideration has been given to the effect of overall temperature difference on heat transfer rate and heat transfer coefficient. The choice of an additional temperature parameter has also been considered.

The behaviour of the system was found to be similar to that of the equivalent linear system. The heat flux density varied almost linearly with the overall temperature difference, and the choice of the additional temperature parameter was found to be largely a matter of convenience. Three possibilities were compared: constant evaporator temperature (appropriate to an isothermal heat source), constant condenser temperature (appropriate to an isothermal heat sink) and constant vapour temperature (appropriate to a constant system pressure).

The thermal performance of the device did not appear to be much affected by the offset length for heat transfer rates below the critical. This offers flexibility to the thermosyphon designer. Under such conditions, heat transfer rates are an order of magnitude higher than in the corresponding single-phase sysem. However, the critical heat fluxes were well below those in the equivalent linear, evaporative system suggesting that the offset length may play a crucial role in determining the maximum heat transfer rate.

Acknowledgements—This work was undertaken with a research grant from the Natural Sciences and Engineering Research Council of Canada to whom we are indebted. We also wish to thank Mr B. Ceilin and Mr A. Muir, of the Department of Mechanical Engineering, for their technical assistance.

REFERENCES

1. K. C. Cheng and J. P. Zarling, Applications of heat pipes and thermosyphons in cold regions, *Proc. 7th Int. Heat Pipe Conf.*, Minsk (1990).

2. K. Negishi and T. Sawada, Heat transfer performance of an inclined, two-phase closed thermosyphon, *Int. J. Heat Mass Transfer* **26,** 1207–1213 (1983).
3. P. Terdtoon, M. Shiraishi and M. Murakami, Investigation of effect of inclination angle on heat transfer characteristics of closed, two-phase thermosyphon, *Proc. 7th Int. Heat Pipe Conf.*, Minsk (1990).
4. E. D. Waters, Arctic tundra kept frozen by heat pipes, *The Oil and Gas Journal*, 122–125 (1974).
5. Anon, First ship with practical de-icing system, *Zosen* **26**(7), p. 26 (1981).
6. E. Long, *Frozen Assets*. Arctic Foundations Inc. (1984).
7. G. S. H. Lock and D. Ladoon, Natural convection in the cranked thermosyphon, *Int. J. Heat Mass Transfer* **36,** 183–188 (1973).
8. G. S. H. Lock, *The Tubular Thermosyphon*. Oxford University Press (1992).
9. H. Imura, K. Sasaguchi, H. Kozai, H. and S. Numata, Critical heat flux in a closed two-phase thermosyphon, *Int. J. Heat Mass Transfer* **26,** 1181–1188 (1983).
10. G. S. H. Lock and Jialin Fu, Natural convection in the inclined, cranked thermosyphon, *J. Heat Transf.* (in press).